RECONSTRUCTION OF THE SOURCE TERM IN A TIME-FRACTIONAL DIFFUSION EQUATION FROM PARTIAL DOMAIN MEASUREMENT

M. HRIZI, A.A. NOVOTNY, AND R. PRAKASH

Abstract. Time-fractional diffusion equations draw attention of many mathematicians from various fields in the recent past because of its widely known applicable aspects. In this paper, a time-fractional inverse source problem is considered and analyzed through two interconnected streams for a broader understanding. Firstly, we establish the identifiability of this inverse problem by proving the existence of its unique solution with respect to the observed data inside the domain. Later on, in the second phase, our inverse problem is rewritten in its weaker form of a topology optimization problem involving a quadratic mismatch functional enhanced with a regularization term which penalizes the perimeter of the support of the source to be reconstructed. Existence of the minimizer is proved using the classical techniques of calculus of variations. To the end, a noniterative reconstruction algorithm is devised with the help of the topological derivative method. Finally, some numerical experiments are presented to support our findings. To conclude, few remarks are mentioned about the significance and benefits of the use of topological derivatives for the analysis of the problems as considered in this article.

1. Introduction

During the last two decades, the time-fractional diffusion equations (FDEs) have been considered by several authors for different fields of sciences and engineering, particularly the inverse problems of FDEs have attracted wide attention [23]. From a physical viewpoint the FDE is obtained from a fractional Fick law which describes transport processes with long memory. In this paper, we address an inverse source problem governed by the two-dimensional time-fractional diffusion equation. The major difficulty of this inverse problem concerns the unidentifiability of general sources term [24, Section 1.3.1]. More precisely, in that paper, Kian, Soccorsi, Xue and Yamamoto proved that this inverse problem is ill-posed in the sense that the source (to be reconstruct) in its general form cannot be uniquely identified from boundary or local internal observation data. In order to overcome this difficulty, in this article, we propose to write the source term by means of separation of variables. Hence, the main aim is to reconstruct the spatial component (with an unknown support) present in the source term of a time-fractional diffusion equation with the help of internal partial measurements. This problem is motivated by several applications in anomalous diffusion phenomena [5, 10, 15, 28, 40]. More precisely, where anomalous diffusion is seriously concerned with environmental problems, such as evaluating the density of underground contaminants [50].

The reconstruction of the spatial component in the source term of a time-fractional diffusion equation from final observation data or boundary measurements has been the subject of several theoretical and numerical research works. Sakamoto and Yamamoto [38] discussed an inverse problem of determining a spatially varying function of the source

Date: January 10, 2023.

2020 *Mathematics Subject Classification.* 49N45, 35R11, 35Q93, 35C20, 49M15.

Key words and phrases. Inverse source problem, time-fractional diffusion equation, partial domain measurement, topological derivative method, noniterative reconstruction algorithm.

by final overdetermining data, while Wang et al. [44] used a reproducing kernel space method to solve an inverse space-dependent source problem from the final observation data. Then, Wei and Wang [46, 47] proposed a modified quasi-boundary value method for identifying the space-dependent source term with the help of final observation data. Wang et al. [43] used the Tikhonov regularization method and a simplified Tikhonov regularization method to solve the inverse space-dependent problem and established the convergence estimates. Jiang et al. [20, 21] proved the uniqueness for determining the space-dependent source term by the partial interior observation and developed an iterative threshold algorithm. Zhang and Xu [49] determined the space-dependent source term from the Cauchy data at one end $x = 0$ and proposed a numerical method to solve the corresponding inverse problem. Recently, Rundell and Zhang [37] determined a source which is supported in a geometrical domain from external boundary measurements.

Inverse source problems, similar to the ones as mentioned above, arise in many important applications and have received considerable attention recently. The determination of the time-dependent source term in the time-fractional diffusion equation is one such problem, see [27, 39, 45, 48].

In most of the works mentioned above, the proposed geometric reconstruction approaches is based on iterative algorithms with the help of final observation data or boundary measurements. In the present paper, we address the problem of multiple anomalies reconstruction using local internal observation data. More precisely, we aim to reconstruct an unknown space-dependent source term which is supported in $\mathcal{D}^* \subset \Omega$ from a local interior measurement of the associated potential taken within an arbitrary sub-region $\Omega_0 \subset \Omega$, where $\Omega \subset \mathbb{R}^2$. In order to overcome the ill-posedness, the considered inverse problem is reformulated as a topology optimization one where the mass distribution is the unknown variable. The topology optimization consists in minimizing a *least-square* functional enhanced with a regularization term which penalizes the perimeter of the unknown support of the space-dependent source term. This *least-square* functional measures the difference between the observed values and the fitted values provided by the model in the sub-region $\Omega_0 \subset \Omega$. To reconstruct the location, size, shape and number of the mass density distributions in the geometrical domain Ω, we propose an approach based on the second-order topological derivative method. The topological sensitivity analysis is used to estimate the variation of the *least-squares* functional with respect to a finite number of ball-shaped trial anomalies. The second-order topological gradient is exploited to develop an efficient and fast noniterative reconstruction algorithm. The main advantages of our numerical procedure are justified by some numerical experiments. This approach has been successfully implemented for a similar problem [36] where the available data is concentrated on a part of boundary instead of the interior of domain. Therefore, because of the difference in nature of mathematical issues in current paper and [36], the selection of the cost functional is different. Consequently, the whole analysis takes a different course. It is important to add here that, in this paper, we adopted a new computational algorithmic approach according to the current challenges in comparison to [36] in order to obtain better numerical results.

The rest of this paper is organized as follows. Section 2 states the inverse source problem and formulates it as a topology optimization one. In Section 3, we discuss the identifiability issue of the inverse problem, whereas, in Section 4, we introduce some notations and present some theoretical results concerning existence, stability, and regularization property of the considered optimization problem. Then, in Section 5, we present the definitions of first-order and higher-order topological derivatives including an asymptotic expansion of a *least-square* functional with respect to a finite number of circular anomalies. The resulting Newton-type method is presented in Section 6, together with the

associated reconstruction algorithm. Finally, in Section 7, we present numerical examples that demonstrate the effectiveness of the devised reconstruction algorithm.

2. Problem formulation

Let Ω be an open bounded domain in $\mathbb{R}^2$ with sufficiently smooth boundary $\partial\Omega$ and $T > 0$. For a given $0 < \alpha < 1$, by ∂_t^α, we denote the Caputo derivative [25], defined as

$$\partial_t^\alpha g(t) := \frac{1}{\Gamma(1-\alpha)} \int_0^t (t-\tau)^{-\alpha} g'(\tau)\, \mathrm{d}\tau, \qquad 0 < t < T, \tag{2.1}$$

where $g'(\tau)$ is the classical first-order derivative of g with respect to variable τ and

$$\Gamma(z) = \int_0^\infty s^{z-1} e^{-s}\, \mathrm{d}s, \ \text{ for } \Re\{z\} > 0, \tag{2.2}$$

denotes Euler's Gamma function with $\Re\{\cdot\}$ being the real part of $\{\cdot\}$. We consider the following time-fractional diffusion equation with the homogeneous Dirichlet boundary data

$$\left\{ \begin{array}{rcll} \partial_t^\alpha \psi(x,t) - \Delta\psi(x,t) + \psi(x,t) &=& f^*(x)\mu(t), & (x,t) \in \Omega \times (0,T), \\ \psi(x,t) &=& 0, & (x,t) \in \partial\Omega \times (0,T), \\ \psi(x,0) &=& 0, & x \in \Omega. \end{array} \right. \tag{2.3}$$

The source term in (2.3) receives contribution from space and time variables in a decomposed format. The component f^* models the spatial counterpart whereas μ is a temporal one which describes the time evolution pattern. Recall that the model problem in (2.3) is a typical representative of a wide range of time-fractional diffusion equations, which were proposed as a powerful candidate for describing anomalous diffusion phenomena in heterogenous media, see for example, [2, 16] and the references therein.

Let Ω_0 be a nonempty open sub-domain in Ω. The problem, we investigate in this article, is about determining the spatial component of the source term f^* in Ω from internal measurements of ψ in $\Omega_0 \times (0,T)$ such that μ is a given non-null function in $C^1([0,T])$ satisfying $\mu(0) \neq 0$.

Based on the underlying physical motivation as mentioned in the introduction, the spatial component of the source term f^* which needs to be determined, can be modeled here as a mass density distribution, namely,

$$f^* = \chi_{\mathcal{D}^*}, \tag{2.4}$$

where $\chi_{\mathcal{D}^*}$ is the characteristic function of the unknown sub-domain $\mathcal{D}^* \subset \Omega \backslash \overline{\Omega_0}$.

In order to present the considered inverse source problem, we first introduce the set of the admissible solutions. It contains the characteristic functions having the form

$$\mathcal{A}(\Omega) = \Big\{ f \in L^\infty(\Omega) :\ f = \chi_{\mathcal{D}},\ \mathcal{D} \subset \Omega \backslash \overline{\Omega_0} \Big\},$$

where $\mathcal{D}$ is an open set having a uniform Lipschitz boundary $\partial\mathcal{D}$ in the sense of [17, Definition 2.4.5]. For each element $f = \chi_{\mathcal{D}}$ belonging to $\mathcal{A}(\Omega)$, we denote by $u[f]$ the solution to the following boundary value problem

$$\left\{ \begin{array}{rcllll} \partial_t^\alpha u[f] - \Delta u[f] + u[f] &=& f\mu & \text{in} & \Omega \times (0,T), \\ u[f] &=& 0 & \text{on} & \partial\Omega \times (0,T), \\ u[f](.,0) &=& 0 & \text{in} & \Omega. \end{array} \right. \tag{2.5}$$

Assuming that the measured data $\psi_{|_{\Omega_0 \times (0,T)}}$ is known in $\Omega_0 \times (0,T)$ with ψ being the potential related to the actual spatial-dependent source term $f^* = \chi_{\mathcal{D}^*}$, (i.e. ψ solves (2.3)), the inverse problem to be solved consists in finding the spatial component $f^* =$

$\chi_{\mathcal{D}^*} \in \mathcal{A}(\Omega)$ such that the associated potential $u[f]$ is the best possible approximation (in the most appropriate sense) of the measured data in $\Omega_0 \times (0,T)$.

According to this observation, the inverse reconstruction problem can be formulated as a topological optimization one consisting in minimizing the discrepancy

$$J(f) = \int_0^T \Big(\int_{\Omega_0} \Big| u[f] - \psi \Big|^2 \mathrm{d}x \Big) \mathrm{d}t. \tag{2.6}$$

On the other hand, in practical applications the observation data $\psi_{|_{\Omega_0 \times (0,T)}}$ cannot be measured with complete precision: noise is intrinsically attached with any measurement method. Thus, we consider ψ^σ as an internal measured data which is assumed to satisfy the following condition:

$$\Big\| \psi - \psi^\sigma \Big\|_{L^2(\Omega_0 \times (0,T))} \leq \sigma, \tag{2.7}$$

where $\sigma > 0$ is the amplitude of noise in the data.

It is well known that this inverse problem is ill-posed in the sense of Hadamard and the solution is very sensitive to the measured data, which causes severe numerical instabilities. We consider the standard approach to tackle the ill-posedness of the problem via the minimization of the least-square functional with a Tikhonov regularization penalizing the perimeter of the set $\mathcal{D}$. More precisely, we consider

$$\begin{cases} \text{Minimize } \ \mathcal{J}(f) := \displaystyle\int_0^T \Big(\int_{\Omega_0} \Big| u[f] - \psi^\sigma \Big|^2 \mathrm{d}x \Big) \mathrm{d}t + \gamma \mathrm{Per}(\mathcal{D}), \\ \text{subject to } \ f = \chi_{\mathcal{D}} \in \mathcal{A}(\Omega) \ \text{ and } \ u[f] \ \text{ being the solution of } \ (2.5), \end{cases} \tag{2.8}$$

where $\gamma > 0$ represents the regularization parameter and $\mathrm{Per}(\mathcal{D})$ denotes the relative perimeter of $\mathcal{D}$ in Ω which is defined according to the De Giorgi formula

$$\mathrm{Per}(\mathcal{D}) = \sup \Big\{ \int_{\mathcal{D}} \mathrm{div}\ \phi \ \Big| \ \phi \in C_c^1(\Omega, \mathbb{R}^2), \ \|\phi\|_\infty \leq 1 \Big\}, \tag{2.9}$$

where $C_c^1(\Omega, \mathbb{R}^2)$ is the space of continuously differentiable functions with compact support in Ω and $\| \cdot \|_\infty$ is the essential supremum norm.

Remark 1.

(1) *In the two-dimensional case, the scaling property of the perimeter is*

$$Per(\tau\mathcal{D}) = \tau Per(\mathcal{D}) \qquad \text{for every } \tau > 0. \tag{2.10}$$

(2) *In the case of a Lipschitz domain $\mathcal{D}$ the perimeter $Per(\mathcal{D})$ of $\mathcal{D}$ coincides with the 1-dimensional Hausdorff measure $\mathcal{H}(\partial\mathcal{D})$ of $\partial\mathcal{D}$; i.e.*

$$Per(\mathcal{D}) = \mathcal{H}(\partial\mathcal{D}), \tag{2.11}$$

where $\partial\mathcal{D}$ is the topological boundary of $\mathcal{D}$. See, [17] *for details. Moreover, when $Per(\mathcal{D}) = \mathcal{H}(\partial\mathcal{D}) < \infty$, we say that $\mathcal{D}$ has a finite perimeter or is a Cacciopolli set. This latter condition is equivalent to*

$$\mathcal{H}(\partial\mathcal{D} \backslash \partial^*\mathcal{D}) = 0, \tag{2.12}$$

where $\partial^*\mathcal{D}$ is the reduced boundary of the set $\mathcal{D}$ in the De Giorgi sense [12]*. In addition, this condition implies that the perimeter $Per(\mathcal{D})$ coincides with the Total Variation (TV) of the distributional gradient of the characteristic function of $\mathcal{D}$, namely (see, e.g.,* [17, Corollary 2.3.5]*):*

$$Per(\mathcal{D}) = TV\Big(\chi_{\mathcal{D}}, \Omega\Big) = |\nabla\chi_{\mathcal{D}}|(\Omega). \tag{2.13}$$

(3) *It is important to observe that the homogeneous Dirichlet condition is considered in the boundary value problem* (2.3) *just for the sake of simplicity, though the entire analysis of this article also works for any non homogeneous data, with a similar technical analysis. In this case, to obtain an analytical solution of the nonhomogeneous time-fractional diffusion problem* (2.3) *or* (2.5)*, Chen et al.* [9] *proposed an approach based on the separation of variables, where the solution is given in the form of the multivariate Mittag-Leffler function. Later, Jiang et al.* [22] *generalized this result for the multi-term time-fractional diffusion equation.*

3. Identifiability

In this section, we will discuss the identifiability question related to the considered inverse problem. Before that, we recall the unique continuation result of problem (2.3) stated in [20, Theorem 2.6].

Lemma 2. *Let $\Omega_0 \subset \Omega$ be an arbitrarily chosen open sub-domain and v is the solution of the following boundary value problem*

$$\left\{\begin{array}{rcll} \partial_t^\alpha v(x,t) - \Delta v(x,t) + v(x,t) &=& h(x)\nu(t), & (x,t) \in \Omega \times (0,T), \\ v(x,t) &=& 0, & (x,t) \in \partial\Omega \times (0,T), \\ v(x,0) &=& 0, & x \in \Omega. \end{array}\right.$$

Assume that h belongs to the finite energy space $L^2(\Omega)$ and $\nu \in C^1([0,T])$ with $\nu(0) \neq 0$. Then $v = 0$ in $\Omega_0 \times (0,T)$ implies $h = 0$ in Ω.

Now we present the main result of this section, the identifiability of the spatial component f^* in problem (2.3)-(2.4) from the internal observation data.

Theorem 3. *For a given $\mu \in C^1([0,T])$ with $\mu(0) \neq 0$ and a nonempty open sub-domain $\Omega_0 \subset \Omega$, let $f_j^* = \chi_{\mathcal{D}_j^*}$, $j = \{1,2\}$ such that the solutions ψ_j of the problems*

$$\left\{\begin{array}{rcll} \partial_t^\alpha \psi_j - \Delta \psi_j + \psi_j &=& f_j^*\,\mu & in \quad \Omega \times (0,T), \\ \psi_j &=& 0 & on \quad \partial\Omega \times (0,T), \\ \psi_j(.,0) &=& 0 & in \quad \Omega, \end{array}\right. \tag{3.1}$$

satisfy

$$\psi_1 = \psi_2 \quad in\ \Omega_0 \times (0,T), \tag{3.2}$$

then $f_1^* = f_2^*$, i.e. $\mathcal{D}_1^* = \mathcal{D}_2^*$.

Proof. Let $w_{2,1}$ be the difference of ψ_1 from ψ_2, i.e. $w_{2,1} = \psi_2 - \psi_1$, then it is a solution of the boundary value problem

$$\left\{\begin{array}{rcll} \partial_t^\alpha w_{2,1} - \Delta w_{2,1} + w_{2,1} &=& f_{2,1}^* & \text{in} \quad \Omega \times (0,T), \\ w_{2,1} &=& 0 & \text{on} \quad \partial\Omega \times (0,T), \\ w_{2,1}(.,0) &=& 0 & \text{in} \quad \Omega, \end{array}\right.$$

where $f_{2,1}^*(x,t) = \mu(t)\Big(\chi_{\mathcal{D}_2^*}(x) - \chi_{\mathcal{D}_1^*}(x)\Big)$. From (3.2), we have

$$w_{2,1} = 0 \ \text{ in } \Omega_0 \times (0,T).$$

Thus, from Lemma 2, we deduce that

$$\chi_{\mathcal{D}_2^*} - \chi_{\mathcal{D}_1^*} = 0.$$

Hence $\mathcal{D}_2^* = \mathcal{D}_1^*$. □

Remark 4. *In simple words, Theorem 3 indicates the one to one correspondence between the measured data in Ω_0 and the unknown spatial component of the source term f^* which we are interested to reconstruct.*

4. Analysis of the optimization problem

In this section, we present three main theoretical results related to the optimization problem (2.8). The first one is devoted to an existence result of an optimal solution. The second one is concerned with its stability. The last one concerns the convergence of minimizers as $\gamma \to 0$ to the solution of the inverse problem. We start our analysis by introducing some definitions as well as some useful preliminary results.

4.1. **Notations and auxiliary results.** For $1 \leq p < \infty$, let $L^p(\Omega)$, $H_0^1(\Omega)$ and $H^2(\Omega)$ be the usual classical Lebesgue and Sobolev spaces. By $H^\alpha(0,T)$ with $\alpha \in (0,1)$, we denote the Sobolev-Slobodecki space with the norm $\|\cdot\|_{H^\alpha(0,T)}$ defined by (see Adams [3, Chapter VII])

$$\|g\|_{H^\alpha(0,T)} = \Big(\|g\|^2_{L^2(0,T)} + \int_0^T \int_0^T \frac{|g(t)-g(s)|^2}{|t-s|^{1+2\alpha}}\,\mathrm{d}t\mathrm{d}s\Big)^{1/2}.$$

Moreover, for the solution regularity of the forward problem, we define the fractional Sobolev spaces ${}_0H^\alpha(0,T)$ as (see, e.g., Kubica, Ryszewska and Yamamoto [26])

$${}_0H^\alpha(0,T) = \begin{cases} H^\alpha(0,T), & \text{if } 0<\alpha<1/2,\\ \Big\{g \in H^{1/2}(0,T):\ \displaystyle\int_0^T \frac{|g(t)|^2}{t}\mathrm{d}t < \infty\Big\}, & \text{if } \alpha = 1/2,\\ \Big\{g \in H^\alpha(0,T):\ g(0)=0\Big\}, & \text{if } 1/2<\alpha<1. \end{cases}$$

In addition, the norm in ${}_0H^\alpha(0,T)$ is equivalent to

$$\|g\|_{\ {}_0H^\alpha(0,T)} = \begin{cases} \|g\|_{H^\alpha(0,T)}, & 0<\alpha<1,\ \ \alpha\neq 1/2,\\ \Big(\|g\|^2_{H^{1/2}(0,T)} + \displaystyle\int_0^T \frac{|g(t)|^2}{t}\mathrm{d}t\Big)^{1/2}, & \alpha = 1/2. \end{cases}$$

In a Banach space $\mathcal{Y}$, we denote the weak convergence of a sequence $\{\mathcal{X}_n\}_n$ to $\mathcal{X}$ by

$$\mathcal{X}_n \rightharpoonup \mathcal{X} \ \text{ in } \ \mathcal{Y} \ \text{ as } n \to \infty.$$

Now, we need some auxiliary results, which will be used in the sequel.

Definition 5. *(see* [17, Definition 2.4.1]*). For ξ being a unitary vector of $\mathbb{R}^d$, $d \geq 2$, τ a strictly positive real number and $y \in \mathbb{R}^d$, the set defined by*

$$\mathcal{C}(y,\xi,\tau) = \Big\{x \in \mathbb{R}^d:\ \langle x-y,\xi\rangle_{\mathbb{R}^d} \geq \cos(\tau)\|x-y\|_{\mathbb{R}^d} \text{ and } 0<\|x-y\|_{\mathbb{R}^d}<\tau\Big\}$$

is called a cone with vertex y, direction ξ, and dimension τ. Here $\langle .,\ .\rangle_{\mathbb{R}^d}$ is the euclidean scalar product of $\mathbb{R}^d$ and $\|.\|_{\mathbb{R}^d}$ is the associated euclidean norm. Moreover, an open set $\mathcal{O}$ of $\mathbb{R}^d$ verifies the τ-cone property, if for every $x \in \partial\mathcal{O}$, there exists a unitary vector ξ_x in $\mathbb{R}^d$ such that for each $y \in \overline{\mathcal{O}} \cap B(x,\tau)$, $\mathcal{C}(y,\xi_x,\tau) \subset \mathcal{O}$, where $B(x,\tau)$ denotes the open ball with center x and radius τ.

The "cone property" concept was introduced by Chenais [11] in the study of an optimal control problem governed by an elliptic partial differential equation where the control is a bounded set in $\mathbb{R}^d$. Particularly, the existence of the optimal control was obtained with the help of an equivalent between the cone condition and uniform Lipschitz condition. More precisely, Chenais proved that the open sets satisfying the "cone property" are equivalent to the following "uniform Lipschitz sets" (also one can see [17, Theorem 2.4.10]).

Definition 6. *(see* [17, Definition 2.4.5]*). We say that a subset $\mathcal{D}$ of $\mathbb{R}^d$ has a uniform Lipschitz boundary if there are some uniform constants L_0, b, r_0 such that for any point s_0 in the boundary $\partial\mathcal{D}$ there exists an orthonormal system of coordinates with origin at s_0,*

a cylinder $K = \mathcal{B}_{r_0}(s_0) \times (-b, b)$*, and a function* $\varphi : \mathcal{B}_{r_0}(s_0) \to [-b, b]$ *which is Lipschitz, with constant* L_0 *and* $\varphi(0) = 0$ *such that*

$$\partial\mathcal{D} \cap K = \Big\{(x, \varphi(x)) : x \in K\Big\},$$
$$\mathcal{D} \cap K = \Big\{ (x, x_N) \in K : x_N > \varphi(y)\Big\}.$$

Here $\mathcal{B}_{r_0}(s_0)$ *is an open ball of radius* r_0 *centred at* s_0 *in* $\mathbb{R}^{d-1}$.

Definition 7. *(see* [17, Definition 2.2.3]*). Let* $\{D^n\}_{n\geq 1}$ *and* D *be (Lebesgue) measurable sets of* $\mathbb{R}^d$ $(d \in \{2, 3\})$*. It is said that* D^n *converges to* D *in the sense of characteristic functions as* $n \to \infty$ *if*

$$\chi_{D^n} \longrightarrow \chi_D \ \text{ in } L^p_{loc}(\mathbb{R}^d) \ \ \forall p \in [1, +\infty[.$$

Consider the class of domains

$$\mathcal{U}_\tau = \Big\{D \text{ open}, \ D \subset \Omega, \ D \text{ has the } \tau - \text{cone property}\Big\}. \tag{4.1}$$

In the above class of domains, we assume that the real number $\tau > 0$ is fixed. This condition gives the link between the set of the admissible solutions $\mathcal{A}(\Omega)$ and the set of admissible shapes $\mathcal{U}_\tau$. In addition, the set of domains $\mathcal{U}_\tau$ enjoys the following compactness property:

Lemma 8. *(see* [17, Theorem 2.4.10]*). Let* $\{D^n\}_n$ *be a sequence in the class* $\mathcal{U}_\tau$*. Then, up to a subsequence, still labelled by* n*,* D^n *converges to some* $D^* \in \mathcal{U}_\tau$*, in the sense of characteristic functions.*

The well-posedness of the boundary value problem (2.5) is provided by the following lemma.

Lemma 9. *Let* $f \in L^2(\Omega)$*,* $\mu \in L^\infty(0, T)$*, and* $0 < \alpha < 1$*. Then the boundary value problem* (2.5) *admits a unique solution* $u[f]$ *in*

$${}_0H^\alpha(0, T; L^2(\Omega)) \cap L^2(0, T; H^2(\Omega) \cap H^1_0(\Omega)) \cap C([0, T]; L^2(\Omega)).$$

Moreover, there exists a constant $c > 0$ *depending on* Ω*,* T*,* α *and* μ *such that*

$$\Big\|u[f]\Big\|_{H^\alpha(0,T;L^2(\Omega))} + \Big\|u[f]\Big\|_{L^2(0,T;H^2(\Omega))} + \Big\|u[f]\Big\|_{C([0,T];L^2(\Omega))} \leq c\Big\|f\Big\|_{L^2(\Omega)}. \tag{4.2}$$

Proof. The proof of this Lemma is a simple consequence of [20, Lemma 2.4] and [38, Theorem 2.2(i)]. □

Definition 10. *(see* [25]*). Let* $g \in L^2(0, T)$*, then for* $\alpha > 0$ *the Riemann-Liouville left- and right-sided fractional integrals are defined by*

$$J^\alpha_{0+}g(t) = \frac{1}{\Gamma(\alpha)} \int_0^t \frac{g(s)}{(t - s)^{1-\alpha}} \mathrm{d}s, \quad 0 < t \leq T, \tag{4.3}$$

and

$$J^\alpha_{T-}g(t) = \frac{1}{\Gamma(\alpha)} \int_t^T \frac{g(s)}{(t - s)^{1-\alpha}} \mathrm{d}s, \quad 0 < t \leq T, \tag{4.4}$$

respectively. Therefore the Caputo derivative ∂^α_t *can be expressed as*

$$\partial^\alpha_t g(t) = J^{1-\alpha}_{0+} g'(t). \tag{4.5}$$

Lemma 11. *(see* [20, Lemma 4.1]*). For* $0 < \alpha < 1$ *and* $\theta_1, \theta_2 \in L^2(0, T)$*, one has*

$$\int_0^T \Big(J^\alpha_{0+}\theta_1(t)\Big)\theta_2(t) \ \mathrm{d}t = \int_0^T \theta_1(t)\Big(J^\alpha_{T-}\theta_2(t)\Big) \ \mathrm{d}t. \tag{4.6}$$

Lemma 12. *Let $\theta \in {}_0H^\alpha(0,T) \cap C([0,T])$ and $l \in C^1([0,T])$. Then*

$$\int_0^T \Big(\partial_t^\alpha \theta\Big) l \, \mathrm{d}t = \theta(T) J_{T-}^{1-\alpha} l(T) - \theta(0) J_{T-}^{1-\alpha} l(0) - \int_0^T \theta \Big(J_{T-}^{1-\alpha} l\Big)' \, \mathrm{d}t. \tag{4.7}$$

Proof. Let $\{\theta_n\}_n$ be a sequence in $C^\infty([0,T])$ such that $\theta_n \to \theta$ in ${}_0H^\alpha(0,T) \cap C([0,T])$ as $n \to \infty$. Then for each $n = 1, 2, ...$, we apply Lemma 11 and the usual integration by parts to derive

$$\begin{aligned}
\int_0^T \Big(\partial_t^\alpha \theta_n\Big) l \, \mathrm{d}t &= \int_0^T \Big(J_{0+}^{1-\alpha} \theta_n'\Big) l \, \mathrm{d}t = \int_0^T \theta_n' \Big(J_{T-}^{1-\alpha} l\Big) \, \mathrm{d}t \\
&= \Big[\theta_n \Big(J_{T-}^{1-\alpha} l\Big)\Big]_0^T - \int_0^T \theta_n \Big(J_{T-}^{1-\alpha} l\Big)' \, \mathrm{d}t \\
&= \theta_n(T) J_{T-}^{1-\alpha} l(T) - \theta_n(0) J_{T-}^{1-\alpha} l(0) - \int_0^T \theta_n \Big(J_{T-}^{1-\alpha} l\Big)' \, \mathrm{d}t.
\end{aligned}$$

Hence, we get the desired result by passing the limit $n \to \infty$ on both sides of the above equality. □

The uniform Lipschitz boundary condition of the sub-domain $\mathcal{D}$ in the set of admissible solutions $\mathcal{A}(\Omega)$ is relevant for the existence of optimal solutions of the optimization problem (2.8), which will be discussed in the next section.

4.2. **Existence of a minimizer.** This section is concerned with the existence of an optimal solution to the considered problem (2.8). The obtained result is summarized in the following theorem.

Theorem 13. *For any $\psi^\sigma \in L^2(\Omega_0 \times (0;T))$, there exists at least one solution to the minimization problem* (2.8).

Proof. Since the function $\mathcal{J}$ from (2.8) is non-negative, it is clear that $\inf_{f \in \mathcal{A}(\Omega)} \mathcal{J}(f)$ is finite. Therefore, there exists a minimizing sequence $\{f^n = \chi_{\mathcal{D}^n}\}_n \subset \mathcal{A}(\Omega)$ such that

$$\lim_{n\to\infty} \mathcal{J}(f^n) = \inf_{f \in \mathcal{A}(\Omega)} \mathcal{J}(f).$$

From the definition of the set of admissible solutions and the equivalent between the τ-cone property and uniform Lipschitz boundary [17, Theorem 2.4.10], it is obvious that the sequence of sub-domains $\{\mathcal{D}^n\}_n \subset \mathcal{U}_\tau$. Due to the compactness property of $\mathcal{U}_\tau$ mentioned in Lemma 8, there exists $\mathcal{D}^* \in \mathcal{U}_\tau$ and a subsequence, still labelled by n, such that

$$f^n = \chi_{\mathcal{D}^n} \longrightarrow f^* = \chi_{\mathcal{D}^*} \text{ in } L^1(\Omega) \text{ as } n \to \infty.$$

In addition, from the definition of $\mathcal{U}_\tau$ and [17, Theorem 2.4.10], we have $\mathcal{D}^*$ is an open set with uniform Lipschitz boundary $\partial\mathcal{D}^*$. Consequently,

$$f^* = \chi_{\mathcal{D}^*} \in \mathcal{A}(\Omega).$$

Now, we prove that $f^* = \chi_{\mathcal{D}^*}$ is indeed a minimizer to (2.8). For each $n \in \mathbb{N}$, let us consider $u[f^n]$ the solution of the boundary value problem (2.5) with $f = f^n$. From Lemma 9, we can deduce that the sequence $\{u[f^n]\}_n$ is bounded in ${}_0H^\alpha(0,T;L^2(\Omega)) \cap L^2(0,T;H^2(\Omega) \cap H_0^1(\Omega))$. This indicates the existence of some u^* in ${}_0H^\alpha(0,T;L^2(\Omega)) \cap L^2(0,T;H^2(\Omega) \cap H_0^1(\Omega))$ and a sub-sequence of $\{u[f^n]\}_n$, again still denoted by $\{u[f^n]\}_n$, such that

$$u[f^n] \rightharpoonup u^* \text{ in } {}_0H^\alpha(0,T;L^2(\Omega)) \cap L^2(0,T;H^2(\Omega) \cap H_0^1(\Omega)) \text{ as } n \to \infty. \tag{4.8}$$

We claim

$$u^* = u[f^*]. \tag{4.9}$$

On the other hand, the weak variational formulation of (2.5) implies

$$\int_0^T \int_\Omega \Big(\partial_t^\alpha u[f^n]\vartheta + \nabla u[f^n].\nabla\vartheta + u[f^n]\vartheta\Big)\mathrm{d}x\mathrm{d}t = \int_0^T \int_\Omega f^n\mu\vartheta\mathrm{d}x\mathrm{d}t,\ \forall\vartheta \in L^2(0,T;H_0^1(\Omega)). \tag{4.10}$$

Due to (4.8), it follows that

$$\partial_t^\alpha u[f^n] \rightharpoonup \partial_t^\alpha u^* \text{ in } L^2(\Omega\times(0,T)) \text{ as } n\to\infty, \tag{4.11}$$

$$\nabla u[f^n] \rightharpoonup \nabla u^* \text{ in } L^2(\Omega\times(0,T))^2 \text{ as } n\to\infty. \tag{4.12}$$

Now, we pass to the limit as $n\to\infty$ in the above weak formulation of (2.5) to obtain

$$\int_0^T \int_\Omega \Big(\partial_t^\alpha u^*\vartheta + \nabla u^*.\nabla\vartheta + u^*\vartheta\Big)\,\mathrm{d}x\mathrm{d}t = \int_0^T \int_\Omega f^*\mu\vartheta\,\mathrm{d}x\mathrm{d}t, \tag{4.13}$$

for all $\vartheta \in L^2(0,T;H_0^1(\Omega))$. To conclude $u^* = u[f^*]$, it remains to prove that $u^*(.,0) = 0$. From Lemma 9, we have $u[f^n] \in {}_0H^\alpha(0,T;L^2(\Omega)) \cap C([0,T];L^2(\Omega))$ which satisfies the assumption of Lemma 12. Therefore, by taking $\varphi \in C^1([0,T])$ with $J_{T-}^{1-\alpha}\varphi(T) = 0$ and using Lemma 12, we obtain

$$\int_0^T \Big(\partial_t^\alpha u[f^n]\Big)\varphi\,\mathrm{d}t = -u[f^n](.,0)J_{T-}^{1-\alpha}\varphi(0) - \int_0^T u[f^n]\Big(J_{T-}^{1-\alpha}\varphi\Big)'\,\mathrm{d}t. \tag{4.14}$$

Let $\theta \in L^2(\Omega)$ be an arbitrary function. By multiplying the above equation with θ and then integrating it in space variable with the identity $u[f^n](.,0) = 0$ in Ω, we have

$$\int_\Omega \int_0^T \Big(\partial_t^\alpha u[f^n]\Big)\varphi\theta\,\mathrm{d}t\mathrm{d}x = -\int_\Omega \int_0^T u[f^n]\Big(J_{T-}^{1-\alpha}\varphi\Big)'\theta\,\mathrm{d}t\mathrm{d}x. \tag{4.15}$$

Passing n to infinity, from (4.8), one can obtain

$$\int_\Omega \int_0^T \Big(\partial_t^\alpha u^*\Big)\varphi\theta\,\mathrm{d}t\mathrm{d}x = -\int_\Omega \int_0^T u^*\Big(J_{T-}^{1-\alpha}\varphi\Big)'\theta\,\mathrm{d}t\mathrm{d}x. \tag{4.16}$$

On the other hand, we have

$$\int_\Omega \int_0^T \Big(\partial_t^\alpha u^*\Big)\varphi\theta\,\mathrm{d}t\mathrm{d}x = -\int_\Omega u^*(.,0)J_{T-}^{1-\alpha}\varphi(0)\theta\,\mathrm{d}x - \int_\Omega \int_0^T u^*\Big(J_{T-}^{1-\alpha}\varphi\Big)'\theta\,\mathrm{d}t\mathrm{d}x, \tag{4.17}$$

for any $\varphi \in C^1([0,T])$ with $J_{T-}^{1-\alpha}\varphi(T) = 0$ and $\theta \in L^2(\Omega)$. Combining (4.14) and (4.17), we obtain

$$\int_\Omega u^*(.,0)J_{T-}^{1-\alpha}\varphi(0)\theta\,\mathrm{d}x = 0,\ \ \forall\theta \in L^2(\Omega). \tag{4.18}$$

Consequently,

$$u^*(.,0) = 0. \tag{4.19}$$

Therefore, it follows from (4.13)-(4.19) and the definition of weak solutions of (2.5) with $f = f^*$ implies that $u^* = u[f^*]$. Finally, by (4.8), we use the lower semi-continuity of

the L^2-norm and the lower semicontinuity property of the perimeter functional (see [12, Section 5.2.1, Theorem 1]) to conclude

$$\begin{aligned}\mathcal{J}(f^*) &= \Big\|u[f^*]-\psi^\sigma\Big\|^2_{L^2(\Omega_0\times(0,T))}+\gamma\mathrm{Per}(\mathcal{D}^*)\\ &\le \liminf_{n\to\infty}\Big\|u[f^n]-\psi^\sigma\Big\|^2_{L^2(\Omega_0\times(0,T))}+\gamma\liminf_{n\to\infty}\mathrm{Per}(\mathcal{D}^n)\\ &\le \liminf_{n\to\infty}\mathcal{J}(f^n)=\inf_{f\in\mathcal{A}(\Omega)}\mathcal{J}(f).\end{aligned}$$

Therefore, f^* is a minimizer to the minimization problem (2.8). □

From the definition of the set of admissible solutions, we deduce that $\mathcal{A}(\Omega)$ can not be a vector space. Moreover, the set $\mathcal{A}(\Omega)$ is only a closed (not even convex) subset of $L^\infty(\Omega)$. Hence, we wish to remark that the uniqueness of the minimizer (in $\mathcal{A}(\Omega)$) remains an open question.

4.3. **Stability.** In this section, we justify the stability of (2.8), namely, the minimization problem (2.8) is indeed a stabilization of the considered inverse problem with respect to the perturbation in the measured data in $\Omega_0\times(0,T)$). More precisely, let $\{\psi_n^\sigma\}_n$ be a sequence of measurements of ψ^σ in $L^2(\Omega_0\times(0,T))$. For each $n\in\mathbb{N}$, we denote by $f^n=\chi_{\mathcal{D}^n}\in\mathcal{A}(\Omega)$, the solution of the following minimization problem

$$\underset{f\in\mathcal{A}(\Omega)}{\text{Minimize}}\ \mathcal{J}_n(f), \tag{4.20}$$

where the cost function $\mathcal{J}_n$ is defined as

$$\mathcal{J}_n(f):=\int_0^T\Big(\int_{\Omega_0}\Big|u[f]-\psi_n^\sigma\Big|^2\mathrm{d}x\Big)\mathrm{d}t+\gamma\mathrm{Per}(\mathcal{D}). \tag{4.21}$$

In the following theorem, we examine the convergence of the sequence $\{f^n=\chi_{\mathcal{D}^n}\}_n$ when the measured data $\psi_n^\sigma\to\psi^\sigma$ in $L^2(0,T;L^2(\Omega_0))$ as $n\to\infty$.

Theorem 14. *If ψ_n^σ tends to ψ^σ in $L^2(0,T;L^2(\Omega_0))$ as $n\to\infty$, then there exists a subsequence of $\{f^n=\chi_{\mathcal{D}^n}\}_n$, such that*

$$f^{n_k}=\chi_{\mathcal{D}^{n_k}}\to f^*=\chi_{\mathcal{D}^\star}\ \text{ in }\ L^1(\Omega)\ \text{ as } k\to\infty,$$

where $f^*=\chi_{\mathcal{D}^\star}\in\mathcal{A}(\Omega)$ is a minimizer of the optimization problem (2.8)*, with datum ψ^σ.*

Proof. The existence of each $f^n=\chi_{\mathcal{D}^n}$ is guaranteed by Theorem 13. According to Lemma 8, there exists $\mathcal{D}^*\in\mathcal{U}_\tau$ and a sub-sequence, still denoted by $\{\mathcal{D}^n\}_n$, such that

$$f^n=\chi_{\mathcal{D}^n}\to f^*=\chi_{\mathcal{D}^\star}\ \text{ in }\ L^1(\Omega)\ \text{ as } n\to\infty.$$

Now it suffices to show that $f^*=\chi_{\mathcal{D}^*}$ is indeed a minimizer of (2.8). Actually, repeating the same argument as that in the proof of Theorem 13, we can derive the following convergence up to a further sub-sequence still denoted by $\{\mathcal{D}^n\}_n$:

$$u[f^n]\rightharpoonup u[f^*]\ \text{ in }\ L^2(0,T;H^2(\Omega)\cap H_0^1(\Omega))\text{ as } n\to\infty. \tag{4.22}$$

Using the convergence of ψ_n^σ to ψ^σ in $L^2(0,T;L^2(\Omega_0))$ as $n\to\infty$ and from (4.22), we obtain

$$u[f^n]-\psi_n^\sigma\rightharpoonup u[f^*]-\psi^\sigma\ \text{ in }\ L^2(0,T;L^2(\Omega_0))\text{ as } n\to\infty.$$

Consequently, for any $f = \chi_{\mathcal{D}} \in \mathcal{A}(\Omega)$, again by the the lower semi-continuity of the L^2-norm and the lower semi-continuity of the perimeter, we can have

$$\begin{aligned}
\mathcal{J}(f^*) &= \Big\|u[f^*] - \psi^\sigma\Big\|^2_{L^2(\Omega_0\times(0,T))} + \gamma \mathrm{Per}(\mathcal{D}^*) \\
&\leq \liminf_{n\to\infty} \Big\|u[f^n] - \psi^\sigma_n\Big\|^2_{L^2(\Omega_0\times(0,T))} + \gamma \liminf_{n\to\infty} \mathrm{Per}(\mathcal{D}^n) \\
&\leq \liminf_{n\to\infty} \Big(\Big\|u[f^n] - \psi^\sigma_n\Big\|^2_{L^2(\Omega_0\times(0,T))} + \gamma \mathrm{Per}(\mathcal{D}^n)\Big) \\
&\leq \lim_{n\to\infty} \Big(\Big\|u[f] - \psi^\sigma_n\Big\|^2_{L^2(\Omega_0\times(0,T))} + \gamma \mathrm{Per}(\mathcal{D})\Big) \\
&= \Big\|u[f] - \psi^\sigma\Big\|^2_{L^2(\Omega_0\times(0,T))} + \gamma \mathrm{Per}(\mathcal{D}),\ \forall f \in \mathcal{A}(\Omega),
\end{aligned}$$

which verifies that $f^* = \chi_{\mathcal{D}^*}$ is a minimizer of (2.8). □

4.4. **Regularization property.** In this section, we prove that the solution to the optimization problem (2.8) converges as $\gamma \to 0$ to the unique solution of the considered inverse problem defined in Section 2.

Theorem 15. *Assume a solution $f^* = \chi_{\mathcal{D}^*} \in \mathcal{A}(\Omega)$ to the inverse problem corresponding to the datum $\psi_{|\Omega_0\times(0,T)}$ exists. For any $\sigma > 0$ let $\Big(\gamma(\sigma)\Big)_{\sigma>0}$ be such that*

$$\gamma(\sigma) \longrightarrow 0 \ \ \textit{as} \ \ \sigma \to 0. \tag{4.23}$$

Furthermore, let $f^\sigma = \chi_{\mathcal{D}^\sigma}$ be a solution to the optimization problem (2.8) with $\gamma = \gamma(\sigma)$. Then

$$\mathcal{D}^\sigma \to \mathcal{D}^*$$

in the sense of characteristic functions as $\sigma \to 0$.

Proof. For each σ, we denote by $f^\sigma = \chi_{\mathcal{D}^\sigma}$, the solution of the optimization problem (2.8) with $\gamma = \gamma(\sigma)$. By repeating the same argument as that in the proof of Theorem 13, we can extract a subsequence of $\{f^\sigma = \chi_{\mathcal{D}^\sigma}\}_\sigma$, for simplicity again denoted by $\{f^\sigma = \chi_{\mathcal{D}^\sigma}\}_\sigma$, such that

$$f^\sigma = \chi_{\mathcal{D}^\sigma} \to f^0 = \chi_{\mathcal{D}^0} \ \text{ in } \ L^1(\Omega) \ \text{ as } \sigma \to 0, \tag{4.24}$$

for some $f^0 = \chi_{\mathcal{D}^0} \in \mathcal{A}(\Omega)$.

Note that $w_\sigma = u[f^\sigma] - u[f^0]$ is a solution to

$$\left\{\begin{array}{rcll}
\partial_t^\alpha w_\sigma - \Delta w_\sigma + w_\sigma &=& (f^\sigma - f^0)\mu & \text{in} \quad \Omega\times(0,T), \\
w_\sigma &=& 0 & \text{on} \quad \partial\Omega\times(0,T), \\
w_\sigma(.,0) &=& 0 & \text{in} \quad \Omega.
\end{array}\right. \tag{4.25}$$

By taking w_σ as a test function in the weak formulation of the boundary value problem (4.25), we get

$$\int_\Omega \Big(\partial_t^\alpha w_\sigma\Big) w_\sigma \mathrm{d}x + \int_\Omega |\nabla w_\sigma|^2 \mathrm{d}x + \int_\Omega |w_\sigma|^2 \mathrm{d}x = \int_\Omega \Big(f^\sigma - f^0)\mu\, w_\sigma \mathrm{d}x. \tag{4.26}$$

In the other hand, from the Alikhanov inequality [4, Lemma 1], we have

$$\frac{1}{2}\int_\Omega \partial_t^\alpha w_\sigma^2 \mathrm{d}x + \int_\Omega |\nabla w_\sigma|^2 \mathrm{d}x + \int_\Omega |w_\sigma|^2 \mathrm{d}x \leq \Big|\int_\Omega \Big(f^\sigma - f^0)\mu\, w_\sigma \mathrm{d}x\Big|. \tag{4.27}$$

From the Cauchy-Schwarz inequality, we deduce that

$$\begin{aligned}\Big\|w_\sigma\Big\|^2_{H^1(\Omega)} &\leq \|\mu\|_{C^1(0,T)}\Big|\int_\Omega \Big(f^\sigma - f^0\Big)w_\sigma \mathrm{d}x\Big| \\ &\leq \|\mu\|_{C^1(0,T)}\Big\|f^\sigma - f^0\Big\|_{L^2(\Omega)}\Big\|w_\sigma\Big\|_{L^2(\Omega)} \\ &\leq \|\mu\|_{C^1(0,T)}\Big\|f^\sigma - f^0\Big\|_{L^2(\Omega)}\Big\|w_\sigma\Big\|_{H^1(\Omega)}.\end{aligned}$$

Hence,

$$\Big\|w_\sigma\Big\|_{H^1(\Omega)} \leq \|\mu\|_{C^1(0,T)}\Big\|f^\sigma - f^0\Big\|_{L^2(\Omega)}.$$

Consequently,

$$\Big\|u[f^\sigma] - u[f^0]\Big\|_{L^2(0,T;H^1(\Omega))} \leq T\|\mu\|_{C^1(0,T)}\Big\|f^\sigma - f^0\Big\|_{L^2(\Omega)} = T\|\mu\|_{C^1(0,T)}\Big\|f^\sigma - f^0\Big\|^{1/2}_{L^1(\Omega)}.$$

By using the convergence results (4.24), we obtain

$$u[f^\sigma] \to u[f^0] \ \text{ in } \ L^2(0,T;H^1(\Omega)) \ \text{ as } \sigma \to 0. \tag{4.28}$$

Consider the solution $f^* = \chi_{\mathcal{D}^*}$ to the inverse problem corresponding to the measured data $\psi_{|_{\Omega_0\times(0,T)}}$. As $f^\sigma = \chi_{\mathcal{D}^\sigma}$ is a minimizer of the optimization problem (2.8) with $\gamma = \gamma(\sigma)$, we have by the minimization property

$$\begin{aligned}\int_0^T \Big(\int_{\Omega_0}\Big|u[f^\sigma] - \psi^\sigma\Big|^2 \mathrm{d}x\Big)\mathrm{d}t + \gamma \mathrm{Per}(\mathcal{D}^\sigma) &\leq \int_0^T \Big(\int_{\Omega_0}\Big|u[f^*] - \psi^\sigma\Big|^2 \mathrm{d}x\Big)\mathrm{d}t + \gamma \mathrm{Per}(\mathcal{D}^*) \\ &= \int_0^T \Big(\int_{\Omega_0}\Big|\psi - \psi^\sigma\Big|^2 \mathrm{d}x\Big)\mathrm{d}t + \gamma \mathrm{Per}(\mathcal{D}^*).\end{aligned}$$

Consequently, from the condition (2.7), one can deduce that

$$\int_0^T \Big(\int_{\Omega_0}\Big|u[f^\sigma] - \psi^\sigma\Big|^2 \mathrm{d}x\Big)\mathrm{d}t \leq \sigma^2 + \gamma \mathrm{Per}(\mathcal{D}^*). \tag{4.29}$$

Passing to the limit in (4.29) as $\sigma \to 0$, from (4.23), we derive

$$\int_0^T \Big(\int_{\Omega_0}\Big|u[f^\sigma] - \psi^\sigma\Big|^2 \mathrm{d}x\Big)\mathrm{d}t \to 0. \tag{4.30}$$

On the other hand, we have

$$\int_0^T \Big(\int_{\Omega_0}\Big|u[f^\sigma] - \psi\Big|^2 \mathrm{d}x\Big)\mathrm{d}t \leq \int_0^T \Big(\int_{\Omega_0}\Big|u[f^\sigma] - \psi^\sigma\Big|^2 \mathrm{d}x\Big)\mathrm{d}t + \int_0^T \Big(\int_{\Omega_0}\Big|\psi - \psi^\sigma\Big|^2 \mathrm{d}x\Big)\mathrm{d}t.$$

By using the above convergence result (4.30) and the condition (2.7), we obtain

$$\int_0^T \Big(\int_{\Omega_0}\Big|u[f^\sigma] - \psi\Big|^2 \mathrm{d}x\Big)\mathrm{d}t \to 0, \quad \sigma \to 0. \tag{4.31}$$

Using (4.28) and from last relation, we have

$$u[f^0] = \psi \quad \text{in } \ \Omega_0 \times (0,\, T) \tag{4.32}$$

and by the uniqueness of the inverse problem proved in Section 3 this implies $f^0 = f^*$ (i.e. $\mathcal{D}^0 = \mathcal{D}^*$) which concludes the proof. □

Remark 16. *In order to prove that the subdomain $\mathcal{D}^\sigma$ has a finite perimeter in Ω we added the assumption $\frac{\sigma^2}{\gamma(\sigma)}$ is bounded for $\sigma \to 0$ in the previous theorem.*

The aim of introducing the regularization term in (2.8) is to stabilize the reconstruction process. But in practice it is very difficult to address the minimization of (2.8) numerically because of the non-diffierentiability of the cost functional. Therefore, in the current paper, we will use a self-regularized approach based on the topological derivative method which is described in the next section.

5. Sensitivity analysis

The considered inverse problem is rewritten as a topology optimization one. To solve the optimization problem (2.8), we propose a fast and accurate approach based on the topological derivative method [30]. Then, for the sake of completeness of the manuscript, we briefly present in Section 5.1 the basic idea of the topological sensitivity. In Section 5.2, we introduce the asymptotic expansion of some modified Bessel functions. Finally, in Section 5.3, we derive a topological asymptotic expansion of the considered shape functional.

5.1. **Topological sensitivity analysis.** Topological derivatives measure the sensitivity of a given shape function with respect to a small topological perturbations such as the creation of inclusions, cavities, cracks, or source-terms. Mathematically, the topological sensitivity concept is the first term of the asymptotic expansion of such shape functions with respect to the small parameter that measures the size of the introduced perturbation. To present the basic idea of this method, we consider an open and bounded domain $\Omega \subset \mathbb{R}^d$ $(d \in \{2,3\})$ and a non-smooth perturbation confined in a small set $\omega_{\varepsilon,z}$ of size $\varepsilon > 0$ centred at an arbitrary point z of Ω such that $\omega_{\varepsilon,z} \Subset \Omega$. We introduce a characteristic function $x \mapsto \chi(x)$, $x \in \Omega$, associated with the unperturbed domain, namely $\chi = \mathbb{1}_\Omega$. Similarly, we define a characteristic function $x \mapsto \chi_\varepsilon(z,x)$, $x \in \Omega$, associated to the topologically perturbed domain. In the case of a perforation, for instance, $\chi_\varepsilon(z) = \mathbb{1}_\Omega - \mathbb{1}_{\omega_{\varepsilon,z}}$ and the perturbed domain is given by $\Omega_{\varepsilon,z} = \Omega \backslash \overline{\omega_{\varepsilon,z}}$. Then, for a given shape functional $\mathcal{F}(\chi_\varepsilon(z))$ associated with the topologically perturbed domain, the topological sensitivity analysis method would provide an asymptotic expansion of $\mathcal{F}(\chi_\varepsilon(z))$ of the form

$$\mathcal{F}(\chi_\varepsilon(z)) = \mathcal{F}(\chi) + f_1(\varepsilon)\mathcal{T}(z) + o(f_1(\varepsilon)), \tag{5.1}$$

where $\mathcal{F}(\chi)$ is the shape functional associated to the reference (unperturbed) domain, $\varepsilon \mapsto f_1(\varepsilon)$ is a positive first order correction scalar function of $\mathcal{F}$, and $o(f_1(\varepsilon))$ is the remainder, namely $o(f_1(\varepsilon))/f_1(\varepsilon) \to 0$ when $\varepsilon \to 0$. The function $z \mapsto \mathcal{T}(z)$ is called the topological derivative (or topological sensitivity) of the shape functional $\mathcal{F}$ at z. Therefore, this derivative can be seen as a first-order correction of $\mathcal{F}(\chi_\varepsilon(z))$ to approximate $\mathcal{F}(\chi)$. In fact, after rearranging (5.1), we have

$$\frac{\mathcal{F}(\chi_\varepsilon(z)) - \mathcal{F}(\chi)}{f_1(\varepsilon)} = \mathcal{T}(z) + \frac{o(f_1(\varepsilon))}{f_1(\varepsilon)}. \tag{5.2}$$

The limit passage $\varepsilon \to 0$ in (5.2) leads to the general definition for the first-order topological derivative

$$\mathcal{T}(z) := \lim_{\varepsilon \to 0} \frac{\mathcal{F}(\chi_\varepsilon(z)) - \mathcal{F}(\chi)}{f_1(\varepsilon)}.$$

This first definition of the topological derivative has been introduced by Schumacher [41] under the name of *bubble method* in the context of compliance optimization for linear elasticity problems, followed by Sokołowski and Żochowski [42] and Céa *et al.* [8]. For more details about this concept, we refer the readers to [34] and references therein as well as to the series of three review papers [31, 32, 33].

Classically, the topological derivative $\mathcal{T}$ is described by the leading term of the first-order asymptotic expansion, dealing only with small geometry perturbations. Therefore, as a natural extension of the topological derivative concept, we consider high-order terms in the asymptotic expansion. In this context, some reconstruction problems have been solved with the help of higher-order topological derivatives [7, 13, 14]. In particular, the shape functional governing the inverse problem is expanded asymptotically with respect to a set of ball-shaped anomalies and then truncated up to some desired order term. Then, an asymptotic expansion of the functional $\mathcal{F}$ at z can be written in the following form

$$\mathcal{F}(\chi_\varepsilon(z)) = \mathcal{F}(\chi) + f_1(\varepsilon)\mathcal{T}(z) + f_2(\varepsilon)\mathcal{T}^2(z) + o(f_2(\varepsilon)), \tag{5.3}$$

where $\varepsilon \mapsto f_2(\varepsilon)$ is a scalar positive function such that $f_2(\varepsilon) = o(f_1(\varepsilon))$ and $f_2(\varepsilon) \to 0$ when $\varepsilon \to 0$ and the function $z \mapsto \mathcal{T}^2(z)$ denotes the second-order topological derivative of the shape function $\mathcal{F}$ at z, which can be defined as

$$\mathcal{T}^2(z) := \lim_{\varepsilon \to 0} \frac{\mathcal{F}(\chi_\varepsilon(z)) - \mathcal{F}(\chi) - f_1(\varepsilon)\mathcal{T}(z)}{f_2(\varepsilon)}.$$

Furthermore, one can define higher-order topological derivatives by arguing analogously.

In this paper, we derive a second-order topological asymptotic expansion for the considered least-square function $\mathcal{J}$ from (2.8) with respect to the presence of a finite number of balls. To this end, we need to introduce the asymptotic expansion of some modified Bessel functions.

5.2. **Series expansions for Bessel functions.** We denote the modified Bessel functions of the first kind and order m by I_m with $m \in \mathbb{Z}$. As $\tau \to 0^+$, we have the following asymptotic expansions:

$$I_0(\tau) = 1 + \frac{1}{4}\tau^2 + O(\tau^4) \tag{5.4}$$

and

$$I_1(\tau) = \frac{1}{2}\tau + \frac{1}{16}\tau^3 + O(\tau^5). \tag{5.5}$$

The modified Bessel functions of the second kind and order m are denoted by K_m with $m \in \mathbb{Z}$. As $\tau \to 0^+$, we have the following asymptotic expansions:

$$K_0(\tau) = (\ln 2 - \mathrm{e}) - \ln \tau - \frac{1}{4}\tau^2 \ln \tau + \frac{1}{4}(1 + \ln 2 - \mathrm{e})\tau^2 + O(\tau^4) \tag{5.6}$$

and

$$K_1(\tau) = \frac{1}{\tau} + \frac{1}{2}\tau \ln \tau + \frac{1}{2}(\mathrm{e} - \ln 2 - \frac{1}{2})\tau + \frac{1}{16}\tau^3 \ln \tau + \frac{1}{16}(\mathrm{e} - \ln 2 - \frac{5}{4})\tau^3 + O(\tau^5), \tag{5.7}$$

where e is the Euler constant. The above series expansions were obtained from Jeffrey et al. [19].

5.3. **Topological asymptotic expansion.** The problem is perturbed by introducing balls in order to determine the sensitivities. More precisely, for a given spatial component in the source term of the time-fractional diffusion equation (2.5) of the form

$$f = \chi_{\mathcal{D}}, \tag{5.8}$$

we consider n ball-shaped perturbations of f denoted by $\bigcup_{i=1}^{n} \mathcal{B}_{\varepsilon_i}(z_i)$, with radii $\varepsilon = (\varepsilon_1, ..., \varepsilon_n)$ and centers $\zeta = (z_1, ..., z_n)$. Since $\mu(t)$ is known, for the sake of completeness it is assumed to be given in the form of piecewise functions in which each component $\mu_i(t)$ is associated with $\mathcal{B}_{\varepsilon_i}(z_i)$, for $i = 1, \cdots, n$, where $\mathcal{B}_{\varepsilon_i}(z_i)$ denotes a ball of radius ε_i and

center $z_i \in \Omega$. In addition, now for the sake of simplicity, we assume that the perturbed counterpart of the source term in the time-fractional diffusion problem (2.5) is defined as

$$F_\varepsilon(x,t) = f(x)\mu(t) + \sum_{i=1}^{n} \rho_i \chi_{\mathcal{B}_{\varepsilon_i}(z_i)}(x), \tag{5.9}$$

where $\rho_i \in \mathbb{R}^+$ is associated with the mean value of $\mu_i(t)$, namely

$$\rho_i = \frac{1}{T}\int_0^T \mu_i(t)\mathrm{d}t. \tag{5.10}$$

Moreover, we assume that $\overline{\mathcal{B}_{\varepsilon_i}(z_i)} \subset \Omega$, $\overline{\mathcal{B}_{\varepsilon_i}(z_i)} \cap \Omega_0 = \emptyset$ and $\mathcal{B}_{\varepsilon_i}(z_i) \cap \mathcal{B}_{\varepsilon_j}(z_j) = \emptyset$ for each $i \neq j$ and $i, j \in \{1, ..., n\}$. The motivation for the choice (5.9) will be explained in what follows.

For the crucial regularization issue presented in this paper, recently, the topological derivative method (particularly for L^2-norm misfit function) has repeatedly been noticed to be self-regularizing, which means they do not need an additional regularization (in the numerical reconstruction) to stabilize the identification process [1, 18, 29]. This feature still needs to be mathematically proven. On the other hand, we know that the perimeter is not topologically differentiable. From the above discussion, we neglect the regularization term in (2.8). Practically, we cannot identify domains having infinite perimeter. Therefore, for the sake of simplicity, we assume that $\mathrm{Per}(\mathcal{D}) < \infty$ and we choose $\gamma = 0$.

To this end, the shape functional associated with the topologically perturbed source term (5.9) is written as

$$\mathcal{J}(F_\varepsilon) = \int_0^T \Big(\int_{\Omega_0} \Big| u_\varepsilon - \psi^\sigma \Big|^2 \mathrm{d}x \Big) \mathrm{d}t, \tag{5.11}$$

where u_ε is solution of the perturbed boundary value problem of the form

$$\left\{ \begin{array}{rcll} \partial_t^\alpha u_\varepsilon - \Delta u_\varepsilon + u_\varepsilon &=& F_\varepsilon & \text{in} \quad \Omega \times (0,T), \\ u_\varepsilon &=& 0 & \text{on} \quad \partial\Omega \times (0,T), \\ u_\varepsilon(.,0) &=& g_\varepsilon & \text{in} \quad \Omega. \end{array} \right. \tag{5.12}$$

From these elements, we will establish an asymptotic formula describing the variation of $\mathcal{J}(F_\varepsilon) - \mathcal{J}(f)$ with respect to ε. Then, let us introduce the following ansatz for the solution to the perturbed problem (5.12):

$$u_\varepsilon(x,t) = u[f](x,t) + \sum_{i=1}^{n} \rho_i \pi \varepsilon_i^2 v_{\varepsilon_i}(x), \tag{5.13}$$

where $u[f]$ solves the homogeneous problem (2.5) and v_{ε_i} is the solution of the following auxiliary boundary value problem for $i = 1, \cdots, n$:

$$\left\{ \begin{array}{rcll} -\Delta v_{\varepsilon_i} + v_{\varepsilon_i} &=& \frac{1}{\pi\varepsilon_i^2}\chi_{\mathcal{B}_{\varepsilon_i}(z_i)} & \text{in} \quad \Omega, \\ v_{\varepsilon_i} &=& 0 & \text{on} \quad \partial\Omega. \end{array} \right. \tag{5.14}$$

Finally, the ansatz (5.13) induces the initial condition $g_\varepsilon(x) = \sum_{i=1}^n \rho_i \pi \varepsilon_i^2 v_{\varepsilon_i}(x)$ to the perturbed boundary value problem (5.12).

Remark 17. *Note that thanks to the construction* (5.9)*, the resulting auxiliary functions* v_{ε_i} *are solutions to steady-state boundary value problems* (5.14)*. From one side, it reduces enormously the computational cost of the algorithm. One the other hand, we will show that we can estimate – with a good precision – the volume* $\rho_i \pi \varepsilon_i^2$ *of each anomaly and its location* z_i*, but not* $\mu_i(t)$ *itself, where* ρ_i *is given by* (5.10)*.*

Now, let us decompose v_{ε_i}, solution of (5.14), into two parts as follows

$$v_{\varepsilon_i}(x) = p_{\varepsilon_i}(x) + \lambda_3^{\varepsilon_i} q_i(x), \tag{5.15}$$

where p_{ε_i} is solution of the following boundary value problem defined in a big ball $\mathcal{B}_R(z_i) \supset \Omega$ of radius R and centre at z_i:

$$\left\{ \begin{array}{rcll} -\Delta p_{\varepsilon_i} + p_{\varepsilon_i} & = & \frac{1}{\pi\varepsilon_i^2}\chi_{\mathcal{B}_{\varepsilon_i}(z_i)} & \text{in} \quad \mathcal{B}_R(z_i), \\ p_{\varepsilon_i} & = & \lambda_3^{\varepsilon_i} K_0(R) & \text{on} \quad \partial\mathcal{B}_R(z_i). \end{array} \right. \tag{5.16}$$

The above boundary value problem admits the explicit solution (see, for instance, the book by Polyanin, 2002 [35])

$$p_{\varepsilon_i}(x) = \left\{ \begin{array}{ll} \lambda_1^{\varepsilon_i} - \lambda_2^{\varepsilon_i} I_0(\|x - z_i\|) & x \in \mathcal{B}_{\varepsilon_i}(z_i), \\ \lambda_3^{\varepsilon_i} K_0(\|x - z_i\|) & x \in \mathcal{B}_R(z_i) \setminus \overline{\mathcal{B}_{\varepsilon_i}(z_i)}, \end{array} \right. \tag{5.17}$$

where

$$\lambda_1^{\varepsilon_i} = \frac{1}{\pi\varepsilon_i^2}, \tag{5.18}$$

$$\lambda_2^{\varepsilon_i} = \frac{1}{\pi\varepsilon_i^2} \frac{K_1(\varepsilon_i)}{K_0(\varepsilon_i)I_1(\varepsilon_i) + K_1(\varepsilon_i)I_0(\varepsilon_i)}, \tag{5.19}$$

and

$$\lambda_3^{\varepsilon_i} = \frac{1}{\pi\varepsilon_i^2} \frac{I_1(\varepsilon_i)}{K_0(\varepsilon_i)I_1(\varepsilon_i) + K_1(\varepsilon_i)I_0(\varepsilon_i)}. \tag{5.20}$$

Finally, $\lambda_3^{\varepsilon_i} q_i$ must compensate for the discrepancies left by p_{ε_i} on $\partial\Omega$. In particular, q_i is the solution to the following boundary value problem

$$\left\{ \begin{array}{rcll} -\Delta q_i + q_i & = & 0 & \text{in } \Omega, \\ q_i & = & -K_0(\|x - z_i\|) & \text{on } \partial\Omega. \end{array} \right. \tag{5.21}$$

Since $\mathcal{B}_{\varepsilon_i}(z_i) \cap \Omega_0 = \emptyset$, then

$$v_{\varepsilon_i}(x) = \lambda_3^{\varepsilon_i} v_i(x) \quad \forall x \in \Omega_0, \tag{5.22}$$

with

$$v_i(x) := q_i(x) + K_0(\|x - z_i\|). \tag{5.23}$$

Consequently, from (5.13) and (5.22), we have the following expansion:

$$u_\varepsilon(x,t) = u[f](x,t) + \sum_{i=1}^{n} \lambda^{\varepsilon_i} v_i(x) \qquad \forall x \in \Omega_0. \tag{5.24}$$

with λ^{ε_i} given by

$$\lambda^{\varepsilon_i} = \rho_i \frac{I_1(\varepsilon_i)}{K_0(\varepsilon_i)I_1(\varepsilon_i) + K_1(\varepsilon_i)I_0(\varepsilon_i)}. \tag{5.25}$$

By using (5.24) in (5.11), we get the following asymptotic expansion:

$$\mathcal{J}(F_\varepsilon) - \mathcal{J}(f) = 2\sum_{i=1}^{n} \lambda^{\varepsilon_i} \int_{\Omega_0} v_i \left(\int_0^T (u[f] - \psi^\sigma) \mathrm{d}t \right) \mathrm{d}x \tag{5.26}$$

$$+ T \sum_{i,j=1}^{n} \lambda^{\varepsilon_i} \lambda^{\varepsilon_j} \int_{\Omega_0} v_i v_j \, \mathrm{d}x. \tag{5.27}$$

6. Reconstruction algorithm

Following the original ideas presented in [6], in this section we present the resulting noniterative reconstruction algorithm based on the expansion (5.26). The topological asymptotic expansion of the cost function $\mathcal{J}(F_\varepsilon)$ given by (5.26) can be rewritten in the following compact form

$$\mathcal{J}(F_\varepsilon) = \mathcal{J}(f) + \Psi(\beta, \zeta, n),$$

where the quantity $\Psi(\beta, \zeta, n)$ is defined by

$$\Psi(\beta, \zeta, n) = \beta \cdot d(\zeta) + \frac{1}{2} H(\zeta)\beta \cdot \beta, \tag{6.1}$$

where vectors $\zeta = (z_1, \cdots, z_n)$ and $\beta = (\beta_1, \cdots \beta_n)$, with $\beta_i = \lambda^{\varepsilon_i}$. Moreover, $d(\zeta)$ and $H(\zeta)$ are the first and second order topological derivatives, respectively. The vector $d(\zeta)$ and matrix $H(\zeta)$ have entries

$$d(\zeta) = \begin{pmatrix} d_1 \\ d_2 \\ \vdots \\ d_n \end{pmatrix} \quad \text{and} \quad H(\zeta) = \begin{pmatrix} H_{11} & H_{12} & \cdots & H_{1n} \\ H_{21} & H_{22} & \cdots & H_{2n} \\ \vdots & \vdots & \ddots & \vdots \\ H_{n1} & H_{n2} & \cdots & H_{nn} \end{pmatrix}, \tag{6.2}$$

where

$$d_i = 2\int_{\Omega_0} v_i \left(\int_0^T (u[f] - \psi^\sigma) \mathrm{d}t \right) \mathrm{d}x \quad \text{and} \quad H_{ij} = 2T \int_{\Omega_0} v_i v_j \mathrm{d}x. \tag{6.3}$$

Given the general function of form (6.1), the minimum is found when:

$$\langle D_\beta \Psi(\beta, \zeta, n), \eta \rangle = 0 \quad \forall \eta \in \mathbb{R}^n. \tag{6.4}$$

Furthermore, given H_{ij} is symmetric positive definite, the minimum of the function with respect to β is the global minimum. In particular,

$$(H(\zeta)\beta + d(\zeta)) \cdot \eta = 0 \quad \forall \eta \in \mathbb{R}^n \quad \Rightarrow \quad H(\zeta)\beta = -d(\zeta), \tag{6.5}$$

provided that $H = H^\top$. Therefore,

$$\beta = \beta(\zeta) = -H(\zeta)^{-1} d(\zeta), \tag{6.6}$$

such that the quantity β, solving (6.6), becomes a function of the locations ζ. Substituting the solution of (6.6) into $\Psi(\beta, \zeta, n)$, defined by (6.1), the optimal locations $\zeta^\star$ can be obtained from a combinatorial search over the domain Ω. These locations are the solutions to the following minimization problem:

$$\zeta^\star = \underset{\zeta \in X}{\operatorname{argmin}} \left\{ \Psi(\beta(\zeta), \zeta, n) = \frac{1}{2}\beta(\zeta) \cdot d(\zeta) \right\}, \tag{6.7}$$

where X is the set of admissible locations of anomalies. Then, the optimal sources are characterized by $\beta^\star = \beta(\zeta^\star)$. Finally, we can use the asymptotic expansions (5.4)-(5.7) to rewrite $\beta_i = \lambda^{\varepsilon_i}$ from (5.25) as follows:

$$\lambda^{\varepsilon_i} = \frac{\rho_i \pi \varepsilon_i^2}{2\pi} + O(\varepsilon_i^4). \tag{6.8}$$

Therefore, the volume of the i-th anomaly can be approximated by $\rho_i \pi \varepsilon_i^2 \approx 2\pi\beta_i$, where ρ_i is given by (5.10).

7. Numerical results

Let us consider a domain $\Omega = (0,1)\times(0,1)$. The time T is set as $T = 1$. In addition, the temporal part of the source term to be reconstruction $\mu(t)$ is composed by two functions $\mu_1(t)$ and $\mu_2(t)$ of the form

$$\mu_1(t) = \begin{cases} 10, & 0 < t < 0.1, \\ 0, & \text{otherwise}, \end{cases} \quad \text{and} \quad \mu_2(t) = \begin{cases} 5, & 0.2 < t < 0.4, \\ 0, & \text{otherwise}. \end{cases} \tag{7.1}$$

The graphs of functions $t \mapsto \mu_1(t)$ and $t \mapsto \mu_2(t)$ are presented in Figure 1. Note that, according to (5.10), the mean values of functions $\mu_1(t)$ and $\mu_2(t)$ are $\rho_1 = \rho_2 = 1$. This choice simplifies the graphical representation of the results since each unknown is approximated by $2\pi\beta_i \approx \rho_i\pi\varepsilon_i^2$, where ρ_i is given by (5.10). That is to say, it is expected to obtain a value of $2\pi\beta_i$ coinciding with the volume $\rho_i\pi\varepsilon_i^2$ of the i-th anomaly.

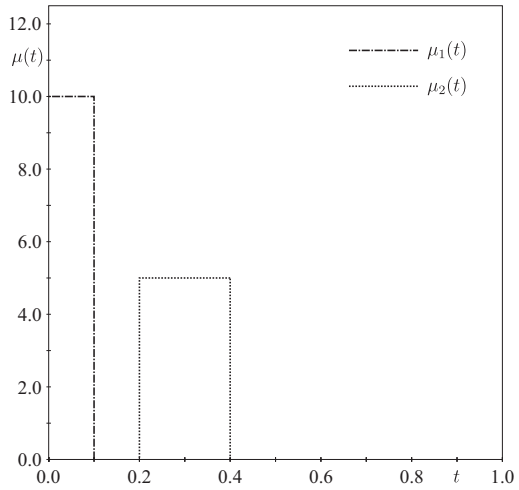

Figure 1. Graphs of functions $t \mapsto \mu_1(t)$ and $t \mapsto \mu_2(t)$.

The problem is discretized by using standard Finite Element Method in space and Finite Difference Method in time following the same procedure as described in [37]. In particular, the domain Ω is discretized with three-node finite elements. The mesh is generated from a grid of size 160×160, where each resulting square is divided into four triangles, leading to 102400 elements. The set X is obtained from a 10×10 uniform subgrid of the initial grid, which results in 100 admissible point locations.

7.1. **Example 1.** In this first example, the source $F^*(x,t)$ to be reconstructed is given by $F^*(x,t) = \mu_1(t)\chi_{\omega_1^*}(x)$, with $\mu_1(t)$ according to (7.1). The domain ω_1^* forming the support of the unknown source $\mathcal{D}^*$ is given by one ball-shaped anomaly, with centre at $(0.6, 0.7)$ and radius 0.05. See Figure 2. In addition, we set $\alpha = 0.5$ and $n = 1$ trial ball. Finally, three different observable domains Ω_0 are considered, all of them given by circles centered at the right-top corner of the square Ω, but with different radii, namely 0.05, 0.025 and 0.02. The obtained results are presented in Figure 3, where the gray region represent the observable domain Ω_0. From this figure, we observe that the reconstruction fails only for the smallest Ω_0, while the reconstructions are almost exact for the bigger observable domains.

7.2. **Example 2.** In this example, the source $F^*(x,t)$ to be reconstructed is given by $F^*(x,t) = \mu_1(t)\chi_{\omega_1^*}(x)+\mu_2(t)\chi_{\omega_2^*}(x)$, with $\mu_1(t)$ and $\mu_2(t)$ according to (7.1). The domains ω_1^* and ω_2^* forming the support of the unknown source $\mathcal{D}^*$ are given by two disjoint ball-shaped anomalies, with centres at $(0.4, 0.4)$, $(0.6, 0.7)$ and radii 0.1, 0.05, respectively. See

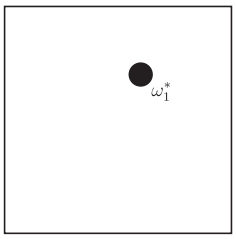

FIGURE 2. Example 1. Target to be reconstruct highlighted in black.

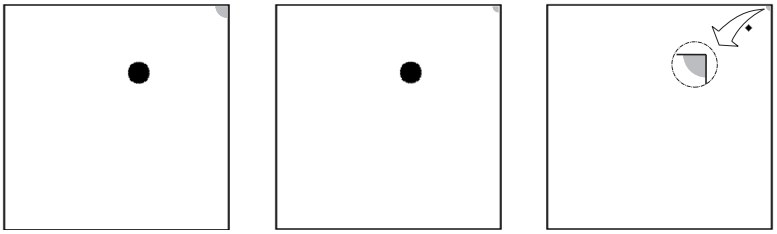

FIGURE 3. Example 1. Obtained results for different observable domains Ω_0 highlighted in gray.

Figure 4, where the gray region represent the observable domain Ω_0 given by four balls with radii 0.1 centered at the corners of Ω.

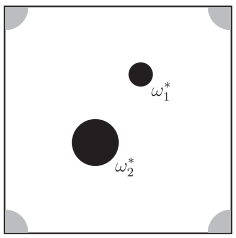

FIGURE 4. Example 2. Target to be reconstruct (black regions) and observable domain (gray regions).

In order to obtain noisy synthetic data, the true source term F^* is corrupted with white Gaussian noise of zero mean and standard deviation σ. See Figure 5. Finally, we set $n = 2$ trial balls and different values of α are considered, namely 0.1, 0.5 and 0.9.

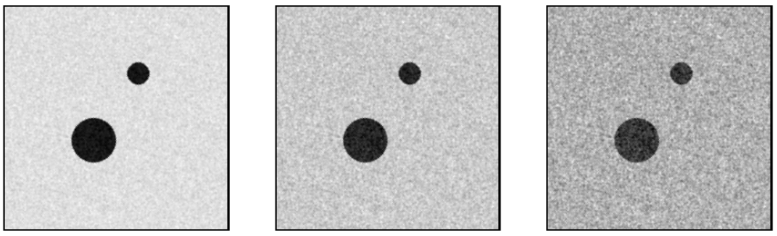

(a) $\sigma = 4\%$ (b) $\sigma = 8\%$ (c) $\sigma = 16\%$

FIGURE 5. Example 2. Target corrupted with varying levels of noise.

The reconstructions for $\sigma = 0\%$ are almost exact independent of α, so that these results are not reported. The obtained results for different levels of noise are presented in Figures 6, 7 and 8 for α equal to 0.1, 0.5 and 0.9, respectively. From an analysis of these figures,

we observe that the smaller is α, the worse is the reconstruction. See also a qualitative summary of the obtained results in Table 1. To complement this analysis, we introduce the following error measure

$$\mathcal{E} = \sum_{i=1}^{2} \|z_i - z_i^*\|^2 + |V_i - V_i^*|, \tag{7.2}$$

where $V_i^* = |\omega_i^*|$ and $V_i = \rho_i \pi \varepsilon_i^2$. Note that, in this particular case, the error measure (7.2) makes sense because each $\mu_i(t)$ has unit mean value in the spirit of (5.10). The obtained errors are reported in Table 2.

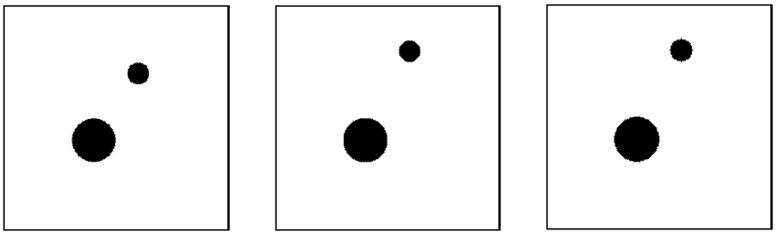

(a) $\sigma = 4\%$ (b) $\sigma = 8\%$ (c) $\sigma = 16\%$

FIGURE 6. Example 2. Obtained result for $\alpha = 0.1$ with varying levels of noise.

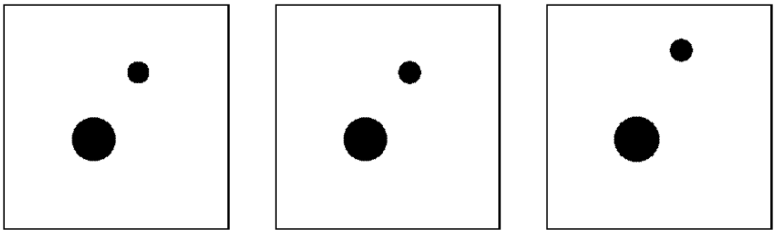

(a) $\sigma = 4\%$ (b) $\sigma = 8\%$ (c) $\sigma = 16\%$

FIGURE 7. Example 2. Obtained result for $\alpha = 0.5$ with varying levels of noise.

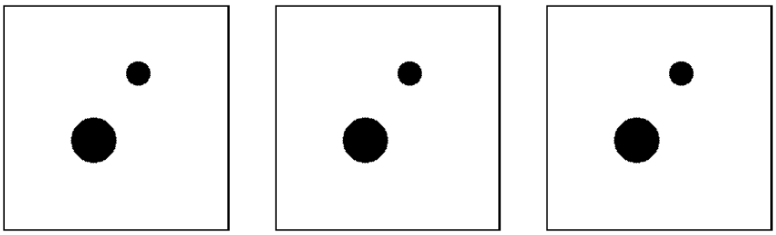

(a) $\sigma = 4\%$ (b) $\sigma = 8\%$ (c) $\sigma = 16\%$

FIGURE 8. Example 2. Obtained result for $\alpha = 0.9$ with varying levels of noise.

TABLE 1. Example 2: Qualitative summary of the obtained results.

	σ	4%	8%	16%
	0.1	good	bad	bad
α	0.5	good	good	bad
	0.9	good	good	good

TABLE 2. Example 2: Error measure $\mathcal{E}$ according to (7.2). The failed reconstructions are highlighted in red.

	σ	4%	8%	16%
	0.1	1.85×10^{-3}	1.06×10^{-2}	1.07×10^{-2}
α	0.5	9.97×10^{-4}	1.16×10^{-3}	1.14×10^{-2}
	0.9	2.77×10^{-4}	3.35×10^{-4}	2.17×10^{-3}

7.3. **Example 3.** Now we consider again the reconstruction of a source term of the form $F^*(x,t) = \mu_1(t)\chi_{\omega_1^*}(x)+\mu_2(t)\chi_{\omega_2^*}(x)$, but with the domains ω_1^* and ω_2^* given by square- and cross-shaped anomalies centered at $(0.6, 0.7)$ and $(0.3, 0.3)$, respectively, where $\mu_1(t)$ and $\mu_2(t)$ are given by (7.1). See Figure 9(a), where the gray regions represent the observable domain Ω_0 given by four tiny balls with radii 0.01 centered at the corners of Ω. We set $\alpha = 0.5$ and $n = 2$ trial balls. The obtained result is reported in Figure 9(b), where we observe that the locations are perfectly reconstructed and the volumes of the target and the trial balls coincide up to a small numerical tolerance.

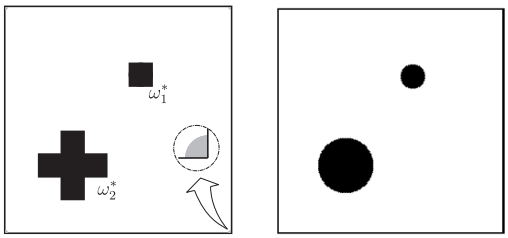

(a) target (b) result

FIGURE 9. Example 3. Target to be reconstruct (black regions) and observable domain (gray regions) on the left (a) and obtained result with $n = 2$ trial balls on the right (b).

7.4. **Example 4.** In this example we consider the reconstruction of a source term of the form $F^*(x,t) = \mu_1(t)\chi_{\omega_1^*}(x) + \mu_2(t)\chi_{\omega_2^*}(x)$, with $\mu_1(t)$ and $\mu_2(t)$ according to (7.1). The domains ω_1^* and ω_2^* are given by ball- and L-shaped anomalies, respectively. See Figure 10(a), where the gray regions represent the observable domain Ω_0 given by four balls with radii 0.05 centered at the corners of Ω. We set $\alpha = 0.5$ and $n = 4$ trial balls. The obtained result is presented in Figure 10(b), where we observe that the target is quite well reconstructed. In particular, the L-shaped anomaly is approximated by three trial balls, while the ball-shaped anomaly is approximated by the fourth trial ball.

7.5. **Example 5.** Finally, let us comeback to Example 2 from Figure 4. However, we consider the reconstruction of a source term of the form $F^*(x,t) = \mu(t)(\chi_{\omega_1^*}(x) + \chi_{\omega_2^*}(x))$, with $\mu(t) = 1 - t$, for $0 < t < 1$. Note that in this case the mean value of $\mu(t)$ is equal to $1/2$. On the other hand, the algorithm returns the volume $\rho_i\pi\varepsilon_i^2$ of the i-th anomaly. Therefore, since $\mu(t)$ is not known a priori, we fix $\rho_i = 1$, for $i = 1, 2$. As a result, after plotting the obtained reconstructions, the size (area) of the true anomalies are under estimated by a factor 2 (up to a small numerical error), as expected. See Figure 11.

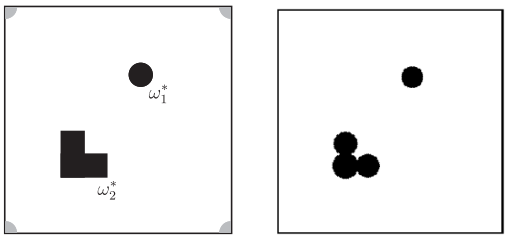

(a) target (b) result

FIGURE 10. Example 4. Target to be reconstruct (black regions) and observable domain (gray regions) on the left (a) and obtained result on the right (b).

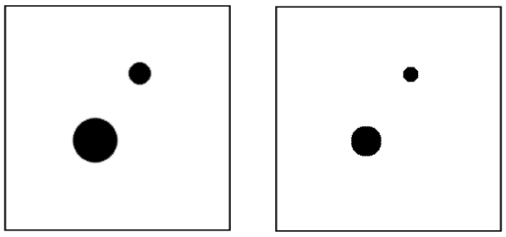

(a) target (b) result

FIGURE 11. Example 5. Target to be reconstruct with $\mu(t) = 1 - t$ on the left (a) and obtained result with $\rho_1 = \rho_2 = 1$ on the right (b).

ACKNOWLEDGEMENT

This research was partly supported by CNPq (Brazilian Research Council), CAPES (Brazilian Higher Education Staff Training Agency) and FAPERJ (Research Foundation of the State of Rio de Janeiro). These financial support are gratefully acknowledged.

REFERENCES

[1] A. B. Abda, M. Hassine, M. Jaoua, and M. Masmoudi. Topological sensitivity analysis for the location of small cavities in stokes flow. *SIAM Journal on Control and Optimization*, 48:2871–2900, 2009.

[2] E.E. Adams and L.W. Gelhar. Field study of dispersion in a heterogeneous aquifer: 2. spatial moments analysis. *Water Resources Research*, 28(12):3293–3307, 1992.

[3] R.A. Adams and J.J.F. Fournier. *Sobolev spaces*. Elsevier, 2003.

[4] A. A. Alikhanov. A priori estimates for solutions of boundary value problems for fractional-order equations. *Differential equations*, 46(5):660–666, 2010.

[5] V.V. Anh, J.M. Angulo, and M.D. Ruiz-Medina. Diffusion on multifractals. *Nonlinear Analysis: Theory, Methods & Applications*, 63(5-7):e2043–e2056, 2005.

[6] A. Canelas, A. Laurain, and A. A. Novotny. A new reconstruction method for the inverse potential problem. *Journal of Computational Physics*, 268:417–431, 2014.

[7] A. Canelas, A. Laurain, and A. A. Novotny. A new reconstruction method for the inverse source problem from partial boundary measurements. *Inverse Problems*, 31(7):075009, 2015.

[8] J. Céa, S. Garreau, Ph. Guillaume, and M. Masmoudi. The shape and topological optimizations connection. *Computer Methods in Applied Mechanics and Engineering*, 188(4):713–726, 2000.

[9] J. Chen, F. Liu, and V. Anh. Analytical solution for the time-fractional telegraph equation by the method of separating variables. *Journal of Mathematical Analysis and Applications*, 338(2):1364–1377, 2008.

[10] W. Chen. A speculative study of 2/3-order fractional laplacian modeling of turbulence: Some thoughts and conjectures. *Chaos: An Interdisciplinary Journal of Nonlinear Science*, 16(2):023126, 2006.

[11] D. Chenais. On the existence of a solution in a domain identification problem. *Journal of Mathematical Analysis and Applications*, 52(2):189–219, 1975.

[12] L. C. Evans. *Measure theory and fine properties of functions*. Routledge, 2018.

[13] L. Fernandez, A. A. Novotny, R. Prakash, and J. Sokołowski. Pollution sources reconstruction based on the topological derivative method. *Applied Mathematics and Optimization*, 84:1493–1525, 2021.

[14] A.D. Ferreira and A. A. Novotny. A new non-iterative reconstruction method for the electrical impedance tomography problem. *Inverse Problems*, 33(3):035005, 2017.

[15] A.A. Greenenko, A.V. Chechkin, and N.F. Shul'Ga. Anomalous diffusion and lévy flights in channeling. *Physics Letters A*, 324(1):82–85, 2004.

[16] Y. Hatano and N. Hatano. On topological derivatives for elastic solids with uncertain input data. *Water resources research*, 34(5):1027–1033, 1998.

[17] A. Henrot and M. Pierre. *Variation et optimisation de formes: une analyse géométrique*, volume 48. Springer Science & Business Media, 2006.

[18] M. Hrizi, A.A. Novotny, and M. Hassine. Imaging of mass distributions from partial domain measurement. *Journal of Inverse and Ill-posed Problems*, 30(5):713–727, 2022.

[19] A. Jeffrey and H.H. Dai. *Handbook of mathematical formulas and integrals*. Elsevier, 2008.

[20] D. Jiang, Z. Li, Y. Liu, and M. Yamamoto. Weak unique continuation property and a related inverse source problem for time-fractional diffusion-advection equations. *Inverse Problems*, 33(5):055013, 2017.

[21] D. Jiang, Y. Liu, and D. Wang. Numerical reconstruction of the spatial component in the source term of a time-fractional diffusion equation. *Advances in Computational Mathematics*, 46(:):1–24, 2020.

[22] H. Jiang, F. Liu, I. Turner, and K. Burrage. Analytical solutions for the multi-term time-fractional diffusion-wave/diffusion equations in a finite domain. *Computers & Mathematics with Applications*, 64(10):3377–3388, 2012.

[23] B. Jin and W. Rundell. A tutorial on inverse problems for anomalous diffusion processes. *Inverse problems*, 31(3):035003, 2020.

[24] Y. Kian, E. Soccorsi, Q. Xue, and M. Yamamoto. Identification of time-varying source term in time-fractional diffusion equations. *Communications in Mathematical Sciences*, 20(1):53—-84, 2022.

[25] A.A. Kilbas, H.M Srivastava, and J.J. Trujillo. *Theory and applications of fractional differential equations*, volume 204. Elsevier, 2006.

[26] A. Kubica, K. Ryszewska, and M. Yamamoto. *Time-fractional Differential Equations: A Theoretical Introduction*. Springer Japan, ToKyo, 2020.

[27] Y.S. Li and T. Wei. An inverse time-dependent source problem for a time-space fractional diffusion equation. *Applied Mathematics and Computation*, 336:257–271, 2018.

[28] M.M. Meerschaert and C. Tadjeran. Finite difference approximations for fractional advection–dispersion flow equations. *Journal of Computational and Applied Mathematics*, 172(1):65–77, 2004.

[29] P. Menoret, M. Hrizi, and A.A. Novotny. On the kohn–vogelius formulation for solving an inverse source problem. *Inverse Problems in Science and Engineering*, 29(1):56–72, 2021.

[30] A. A. Novotny and J. Sokołowski. *Topological derivatives in shape optimization*. Interaction of Mechanics and Mathematics. Springer-Verlag, Berlin, Heidelberg, 2013.

[31] A. A. Novotny, J. Sokołowski, and A. Żochowski. Topological derivatives of shape functionals. Part I: Theory in singularly perturbed geometrical domains. *Journal of Optimization Theory and Applications*, 180(2):341–373, 2019.

[32] A. A. Novotny, J. Sokołowski, and A. Żochowski. Topological derivatives of shape functionals. Part II: First order method and applications. *Journal of Optimization Theory and Applications*, 180(3):683–710, 2019.

[33] A. A. Novotny, J. Sokołowski, and A. Żochowski. Topological derivatives of shape functionals. Part III: Second order method and applications. *Journal of Optimization Theory and Applications*, 181(1):1–22, 2019.

[34] A.A. Novotny and J. Sokołowski. *An introduction to the topological derivative method*. Springer Briefs in Mathematics. Springer Nature Switzerland, 2020.

[35] A. D. Polyanin. *Handbook of linear partial differential equations for engineers and scientists*. Chapman & Hall/CRC, USA, 2002.

[36] R. Prakash, M. Hrizi, and A.A. Novotny. A noniterative reconstruction method for solving a time-fractional inverse source problem from partial boundary measurement. *Inverse Problems*, 38(1):015002, 2021.
[37] W. Rundell and Z. Zhang. Recovering an unknown source in a fractional diffusion problem. *Journal of Computational Physics*, 368:299 – 314, 2018.
[38] K. Sakamoto and M. Yamamoto. Initial value/boundary value problems for fractional diffusion-wave equations and applications to some inverse problems. *Journal of Mathematical Analysis and Applications*, 382(1):426–447, 2011.
[39] K. Sakamoto and M. Yamamoto. Inverse source problem with a final overdetermination for a fractional diffusion equation. *Mathematical Control & Related Fields*, 1(4):509, 2011.
[40] B.M. Schulz and M. Schulz. Numerical investigations of anomalous diffusion effects in glasses. *Journal of non-crystalline solids*, 352(42-49):4884–4887, 2006.
[41] A. Schumacher. *Topologieoptimierung von Bauteilstrukturen unter Verwendung von Lochpositionierungskriterien*. PhD thesis, Forschungszentrum für Multidisziplinäre Analysen und Angewandte Strukturoptimierung. Institut für Mechanik und Regelungstechnik, 1996.
[42] J. Sokołowski and A. Żochowski. On the topological derivative in shape optimization. *SIAM Journal on Control and Optimization*, 37(4):1251–1272, 1999.
[43] J.G. Wang, Y.B. Zhou, and T. Wei. Two regularization methods to identify a space-dependent source for the time-fractional diffusion equation. *Applied Numerical Mathematics*, 68:39–57, 2013.
[44] W. Wang, M. Yamamoto, and B. Han. Numerical method in reproducing kernel space for an inverse source problem for the fractional diffusion equation. *Inverse Problems*, 29(9):095009, 2013.
[45] T. Wei, X.L. Li, and Y.S. Li. An inverse time-dependent source problem for a time-fractional diffusion equation. *Inverse Problems*, 32(8):085003, 2016.
[46] T. Wei and J. Wang. A modified quasi-boundary value method for an inverse source problem of the time-fractional diffusion equation. *Applied Numerical Mathematics*, 78:95–111, 2014.
[47] T. Wei and J.G. Wang. A modified quasi-boundary value method for the backward time-fractional diffusion problem. *ESAIM: Mathematical Modelling and Numerical Analysis*, 48(2):603–621, 2014.
[48] T. Wei and Z.Q. Zhang. Reconstruction of a time-dependent source term in a time-fractional diffusion equation. *Engineering Analysis with Boundary Elements*, 37(1):23–31, 2013.
[49] Y. Zhang and X. Xu. Inverse source problem for a fractional diffusion equation. *Inverse problems*, 27(3):035010, 2011.
[50] L. Zhou and H.M. Selim. Application of the fractional advection-dispersion equation in porous media. *Soil Science Society of America Journal*, 67(4):1079–1084, 2003.

(M. Hrizi) Monastir University, Department of Mathematics, Faculty of Sciences, Avenue de l'Environnement 5000, Monastir, Tunisia
Email address: mourad-hrizi@hotmail.fr

(A.A. Novotny) Laboratório Nacional de Computação Científica LNCC/MCTI, Coordenação de Métodos Matemáticos e Computacionais, Av. Getúlio Vargas 333, 25651-075 Petrópolis - RJ, Brasil
Email address: novotny@lncc.br

(Ravi Prakash) Departamento de Matemática, Facultad de Ciencias Físicas y Matemáticas, Universidad de Concepción, Avenida Esteban Iturra s/n, Bairro Universitario, Casilla 160 C, Concepción, Chile.
Email address: rprakash@udec.cl